

Zeeman splitting in ballistic GaInAs / InP split-gate quantum point contacts

Th. Schäpers, V. A. Guzenko, and H. Hardtdegen

Citation: *Appl. Phys. Lett.* **90**, 122107 (2007); doi: 10.1063/1.2715106

View online: <https://doi.org/10.1063/1.2715106>

View Table of Contents: <http://aip.scitation.org/toc/apl/90/12>

Published by the [American Institute of Physics](#)

Articles you may be interested in

[Fabry-Pérot interference in a triple-gated quantum point contact](#)

Applied Physics Letters **109**, 143509 (2016); 10.1063/1.4964404



Scilight

Sharp, quick summaries **illuminating**
the latest physics research

Sign up for **FREE!**

AIP
Publishing

Zeeman splitting in ballistic GaInAs/InP split-gate quantum point contacts

Th. Schäpers^{a)} and V. A. Guzenko

Institut für Bio- and Nanosysteme (IBN-1) and Virtual Institute of Spinelectronics (VISel), Research Centre Jülich GmbH, 52425 Jülich, Germany

H. Hardtdegen

Institut für Bio- and Nanosysteme (IBN-1) and cni-Center of Nanoelectronic Systems for Information Technology, Research Centre Jülich GmbH, 52425 Jülich, Germany

(Received 23 January 2007; accepted 15 February 2007; published online 20 March 2007)

The Zeeman splitting in ballistic Ga_xIn_{1-x}As/InP split-gate point contacts was investigated. The measurements were performed in a magnetic field perpendicular to the plane of the two-dimensional electron gas. The Zeeman energy splitting between the one-dimensional subbands was determined by measuring the differential conductance as a function of the dc source-drain voltage across the point contact. The g factor of approximately 4.0 extracted from measurements at various magnetic fields agrees well to the value obtained by other methods for this type of heterostructure. © 2007 American Institute of Physics. [DOI: 10.1063/1.2715106]

The generation of spin-polarized currents is one of the key requirements for the realization of semiconducting spin electronic devices.¹ Spin-polarized currents can be generated by injecting carriers from a metallic ferromagnetic electrode or from a diluted magnetic semiconductor.¹ Alternatively, the Zeeman energy splitting in an external magnetic field can also be utilized to create spin-polarized carriers injected from a split-gate point contact.^{2,3} In order to obtain a sufficiently large Zeeman splitting, it is desirable to have access to materials with a large g factor, e.g., InAs-based semiconductors.

Two-dimensional electron gases (2DEGs) based on heterostructures with a Ga_xIn_{1-x}As conductive channel are very interesting for spin electronic applications. One important aspect regarding this material system is that the spin precession can be very well controlled by means of the Rashba effect.^{4,5} In addition, it was recently demonstrated that the electron g factor can be tuned by a gate electrode.⁶ Because of the high mobilities achieved in these heterostructures, ballistic transport has been demonstrated,^{7,8} which is an important prerequisite regarding the creation of spin-polarized currents by means of the Zeeman splitting in split-gate point contacts.

In this letter, we present measurements of the Zeeman spin splitting of one-dimensional subbands in a Ga_xIn_{1-x}As/InP split-gate point contact. The Zeeman energy splitting is determined spectroscopically by measuring the differential conductance as a function of the source-drain bias voltage V_{sd} .⁹⁻¹² This type of measurement has been employed previously to investigate the Zeeman effect on electrons or holes in AlGaAs/GaAs point contacts.¹³⁻¹⁵ In our study the Zeeman energy is directly extracted from the width of the lowest conductance plateau with respect to V_{sd} . The value of the g factor determined from these experiments will be compared to values obtained by alternative approaches.

Our sample is based on a Ga_xIn_{1-x}As/InP heterostructure grown by metal-organic vapor phase epitaxy. The layer system is depicted in Fig. 1 (inset). The 2DEG is located in the strained Ga_{0.23}In_{0.77}As layer. At a temperature of 0.5 K the sheet electron concentration n and mobility μ of the

2DEG are $5.38 \times 10^{11} \text{ cm}^{-2}$ and $230\,000 \text{ cm}^2/\text{V s}$, respectively, resulting in an elastic mean free path l_{el} of $3.1 \mu\text{m}$.

The split-gate point contact structures were fabricated by first defining the mesa structure using reactive ion etching (CH_4/H_2). Subsequently, Ohmic contacts were prepared using a Ni/AuGe/Ni/Au layer system. The gate electrodes of the split-gate point contacts were isolated from the GaInAs surface by a 120-nm-thick hydrogen silsesquioxane layer [see Fig. 1 (inset)]. Finally, the Cr/Au split-gate electrodes were prepared by electron beam lithography and lift-off. The geometrical width of the split-gate opening was 160 nm. An electron beam micrograph of the gate electrodes is shown in Fig. 2(b).

The measurements were performed at a temperature of 0.5 K in a He-3 cryostat with the magnetic field oriented perpendicular to the plane of the 2DEG. The differential conductances $G = dI/dV$ of the point contacts were determined by using an ac current of 20 nA with a superimposed dc current. The ac voltage drop was measured with a lock-in amplifier, while the source-drain voltage V_{sd} resulting from the dc bias current was simultaneously measured using a voltmeter.

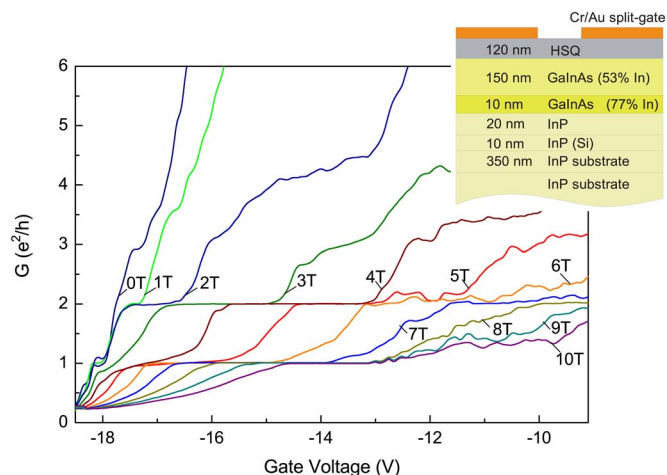


FIG. 1. (Color online) Differential conductance G in units of e^2/h as a function of gate voltage V_g at various magnetic fields B for $V_{sd}=0$. The inset shows a schematic cross section of the split-gate point contact.

^{a)}Electronic mail: th.schaeppers@fz-juelich.de

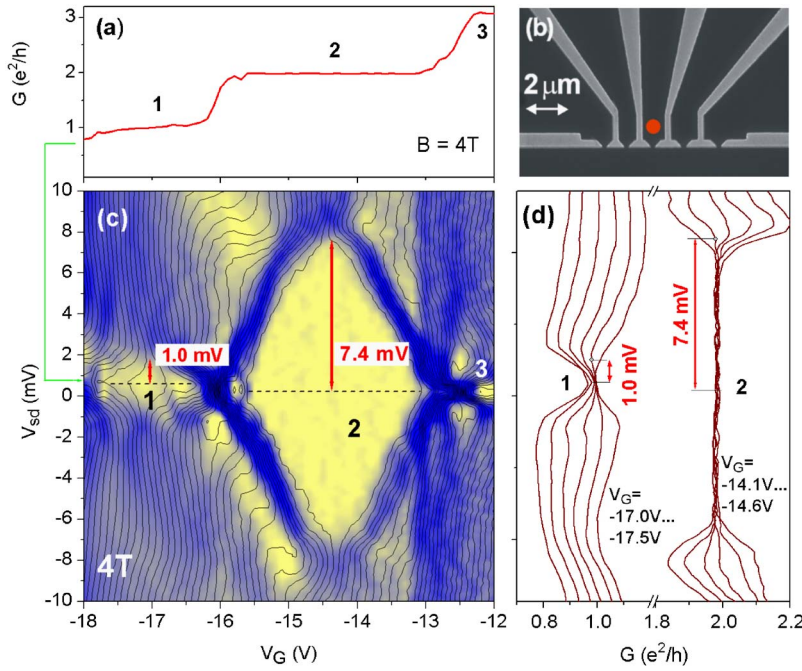


FIG. 2. (Color online) (a) Differential conductance at $V_{sd}=0.8$ mV as a function of gate voltage at a magnetic field of 4 T. (b) Electron beam micrograph of split-gate structures. Only the center point contact, indicated by a dot, was used in the current study. (c) Contour plot of the differential conductance G as a function of bias voltage V_{sd} and gate voltage V_g at 4 T. The corresponding transconductance dG/dV_g is shown as a color scale plot; the light yellow regions correspond to low transconductance regions (conductance plateaus) and the blue regions correspond to high transconductance regions. (d) Differential conductance G as a function of V_{sd} at the center of the first (1) and second (2) plateaus.

The differential conductance G at $V_{sd}=0$ as a function of gate voltage V_g at various magnetic fields B is shown in Fig. 1. At small magnetic fields ($B < 1$ T) no clear quantized conductance is observed which can be attributed to a reduced mean free path due to lower electron concentration in the channel and enhanced scattering due to reduced carrier screening. For magnetic fields $B \geq 1$ T plateaus at $G=e^2/h$ and at $2e^2/h$ are found. The first plateau can be attributed to transport via the lowest Zeeman-split subband, denoted by "1" in Fig. 4 (inset), while the following plateau originates from the transport through the lowest two subbands with opposite spin. The appearance of quantized conductance at finite magnetic fields can be attributed to the improved adiabatic transport¹⁶ and to the increased level separation due to the Landau quantization.¹⁷ In addition, at intermediate magnetic field (4–6 T) plateaus at $3e^2/h$ and $4e^2/h$ are found corresponding to the transport through three and four spin-resolved one-dimensional channels [cf. Fig. 4 (inset)].

In order to gain information on the energetic separation of the one-dimensional subbands, the differential conductance G was measured as a function of V_{sd} and gate voltage. As illustrated in Fig. 4 (inset), by applying V_{sd} the electrochemical potentials of the source (μ_s) and drain (μ_d) contacts are shifted symmetrically in opposite directions with respect to the potential of the point contact constriction.¹⁸ As long as μ_s and μ_d are both in between the minima of two neighboring one-dimensional subbands a conductance plateau at Ne^2/h is expected, corresponding to the total number N of occupied subbands at equilibrium. A deviation from the quantized value of G occurs if V_{sd} is that large that μ_s or μ_d either cross the next higher or the next lower subband level. The subband energy spacing can be obtained directly by determining the maximum value of V_{sd} where the conductance plateau disappears.¹⁰ This corresponds to the situation, where μ_s matches to the minimum of the next higher subband and μ_d matches to the next lower one or vice versa.

Figure 2(c) shows the contour plot of G at $B=4$ T together with the corresponding transconductance dG/dV_g as a color scale plot. As can be seen in Fig. 2(a), clear conductance plateaus at $G=2e^2/h$ and e^2/h are resolved close to

zero source-drain voltage. If the magnitude of V_{sd} is increased as a parameter, the widths of the conductance plateaus decrease. As explained above, the value of V_{sd} at which the plateau vanishes completely is a measure for the subband energy separation. This is the case at 7.4 mV for the second plateau and at 1.0 mV for the first plateau [cf. Figs. 2(c) and 2(d)]. The energy value of 7.4 meV corresponds to the separation of the second and third spin-resolved subbands. This energy separation results from the combined effect of the geometrical constriction confinement and the Landau quantization after subtracting the Zeeman energy $E_z=g\mu_B B$, with μ_B the Bohr magneton. The sublevel separation of 1.0 meV for the first plateau directly corresponds to the Zeeman splitting energy E_z .

By successively increasing the magnetic field, the Zeeman energy splitting increases. This can be seen in Figs. 3(a) and 3(b), where $E_z=1.3$ and 2.0 meV were extracted at a magnetic fields set to 5 and 8 T, respectively. In Fig. 4 the

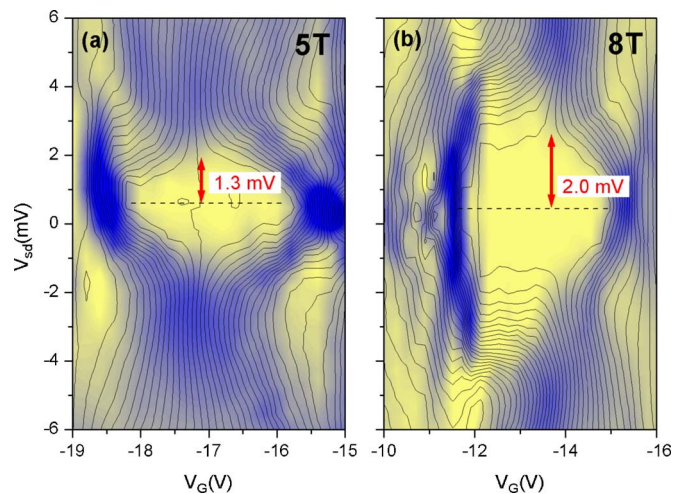


FIG. 3. (Color online) (a) Contour plot of the differential conductance G at $B=5$ T as a function of bias voltage V_{sd} and gate voltage V_g . The corresponding transconductance dG/dV_g is shown as a color scale plot (same scale as used in Fig. 2). (b) Corresponding plot for $B=8$ T.

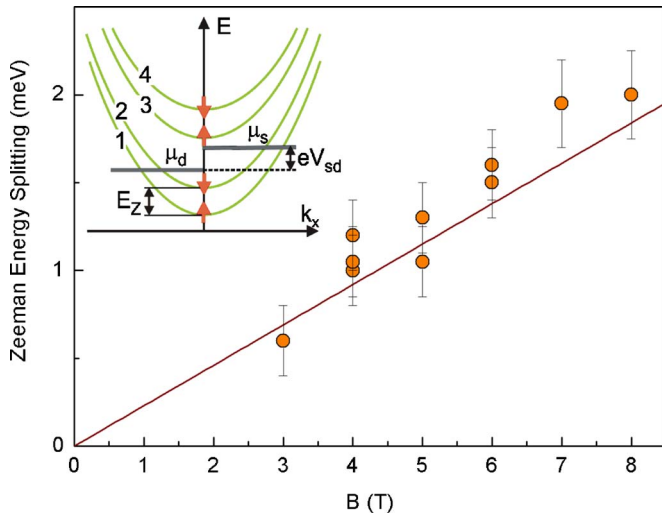


FIG. 4. (Color online) Zeeman energy splitting as a function of magnetic field (dots). The full line corresponds to the calculated Zeeman splitting assuming a g factor of 4.0. The inset illustrates the energy dispersion of the point contact.

Zeeman energy splitting E_z determined from the width of the last conductance plateau with respect to V_{sd} is plotted as a function of B . Using the coincidence method,¹⁹ a value of $g=4.0\pm0.2$ was determined for our heterostructure by performing Shubnikov-de Haas measurements on Hall bar samples at tilted magnetic fields. This value agrees well to reported g factors ranging from 3 to 4 for comparable $\text{Ga}_x\text{In}_{1-x}\text{As}/\text{InP}$ heterostructures.^{20–22} As a reference the Zeeman splitting E_z for $g=4$ is plotted in Fig. 4. The values of E_z extracted from our measurements correspond reasonably well to this curve. However, a closer look reveals that except for two values all data points of E_z determined from the point contact measurements are above the curve corresponding to $g=4$. This might be an indication for an enhanced Zeeman splitting in one-dimensional systems.^{14,23–25}

In conclusion, the Zeeman energy splitting between one-dimensional subbands in a $\text{Ga}_x\text{In}_{1-x}\text{As}/\text{InP}$ split-gate point contact was determined by measuring the differential conductance as a function of V_{sd} . Owing to the large g factor of approximately 4, Zeeman splitting between the subbands was resolved at fields as low as 1 T. At 8 T a Zeeman splitting as large as 2 meV has been observed. Owing to the large g factor, the spin splitting obtained in our structures is substantially larger than in split-gate point contacts based on conventional $\text{AlGaAs}/\text{GaAs}$ heterostructures.¹⁴ Because of

the pronounced Zeeman splitting, $\text{Ga}_x\text{In}_{1-x}\text{As}/\text{InP}$ split-gate point contacts are very attractive as injectors for ballistic spin-polarized electrons.

- ¹I. Zutic, J. Fabian, and S. D. Sarma, *Rev. Mod. Phys.* **76**, 323 (2004).
- ²R. Potok, J. Folk, C. Marcus, and V. Umansky, *Phys. Rev. Lett.* **89**, 266602 (2002).
- ³S. K. Watson, R. M. Potok, C. M. Marcus, and V. Umansky, *Phys. Rev. Lett.* **91**, 258301 (2003).
- ⁴J. Nitta, T. Akazaki, H. Takayanagi, and T. Enoki, *Phys. Rev. Lett.* **78**, 1335 (1997).
- ⁵G. Engels, J. Lange, Th. Schäpers, and H. Lüth, *Phys. Rev. B* **55**, R1958 (1997).
- ⁶J. Nitta, Y. Lin, T. Akazaki, and T. Koga, *Appl. Phys. Lett.* **83**, 4565 (2003).
- ⁷M. F. Tietze, Th. Schäpers, J. Appenzeller, G. Engels, M. Hoffelder, B. Lengeler, and H. Lüth, *J. Appl. Phys.* **79**, 871 (1996).
- ⁸D. Uhlisch, J. Appenzeller, M. F. Tietze, Th. Schäpers, M. Hoffelder, and H. Lüth, *Phys. Rev. B* **57**, 1834 (1998).
- ⁹L. P. Kouwenhoven, B. J. van Wees, C. J. P. M. Harmans, J. G. Williamson, H. van Houten, C. W. J. Beenakker, C. T. Foxon, and J. J. Harris, *Phys. Rev. B* **39**, 8040 (1989).
- ¹⁰N. K. Patel, J. T. Nicholls, L. Martin-Moreno, M. Pepper, J. E. F. Frost, D. A. Ritchie, and G. A. C. Jones, *Phys. Rev. B* **44**, 13549 (1991).
- ¹¹K. S. Pyshkin, C. J. B. Ford, R. H. Harrell, M. Pepper, E. H. Linfield, and D. A. Ritchie, *Phys. Rev. B* **62**, 15842 (2000).
- ¹²S. F. Fischer, G. Apetrii, U. Kunze, D. Schuh, and G. Abstreiter, *Nat. Phys.* **2**, 91 (2006).
- ¹³R. Danneau, O. Klochan, W. R. Clarke, L. H. Ho, A. P. Micolich, M. Y. Simmons, A. R. Hamilton, M. Pepper, D. A. Ritchie, and U. Zülicke, *Phys. Rev. Lett.* **97**, 026403 (2006).
- ¹⁴K. J. Thomas, J. T. Nicholls, N. J. Appleyard, M. Y. Simmons, M. Pepper, D. R. Mace, W. R. Tribe, and D. A. Ritchie, *Phys. Rev. B* **58**, 4846 (1998).
- ¹⁵A. J. Daneshvar, C. J. B. Ford, A. R. Hamilton, M. Y. Simmons, M. Pepper, and D. A. Ritchie, *Phys. Rev. B* **55**, R13409 (1997).
- ¹⁶L. I. Glazman and M. Johnson, *J. Phys.: Condens. Matter* **1**, 5547 (1989).
- ¹⁷K. F. Berggren, T. J. Thornton, D. J. Newson, and M. Pepper, *Phys. Rev. Lett.* **57**, 1769 (1986).
- ¹⁸L. I. Glazman and A. V. Khaetskii, *Europhys. Lett.* **9**, 263 (1989).
- ¹⁹F. F. Fang and P. J. Stiles, *Phys. Rev.* **174**, 823 (1968).
- ²⁰D. L. Vehse, S. G. Hummel, H. M. Cox, F. DeRosa, and S. J. Allen, *Phys. Rev. B* **33**, 5862 (1986).
- ²¹M. Dobers, J. P. Vieren, Y. Guldner, P. Bove, F. Omnes, and M. Razeghi, *Phys. Rev. B* **40**, 8075 (1989).
- ²²I. G. Savel'ev, A. M. Kreshchuk, S. V. Novikov, A. Y. Shik, G. Remenyi, G. Kovacs, B. Podor, and G. Gombos, *J. Phys.: Condens. Matter* **8**, 9025 (1996).
- ²³R. Kotlyar, T. L. Reinecke, M. Bayer, and A. Förchel, *Phys. Rev. B* **63**, 085310 (2001).
- ²⁴I. Pallecchi, Ch. Heyn, J. Lohse, B. Kramer, and W. Hansen, *Phys. Rev. B* **65**, 125303 (2002).
- ²⁵A. Struck, S. Mohammadi, S. Kettemann, and B. Kramer, *Phys. Rev. B* **72**, 245317 (2005).